Available online at www.sciencedirect.com
SCIENCE DIRECT®
Inorganica Chimica Acta 359 (2006) 800–806
Inorganica Chimica Acta
www.elsevier.com/locate/ica

Synthesis, characterization and reactivity of polypyridyl ruthenium(II) carbonyl complexes with phosphine derivatives: Ruthenium–carbon bond labilization based on steric and electronic effects

Dai Ooyama [a,*], Madoka Saito [b]

[a] Department of Industrial Systems Engineering, Cluster of Science and Technology, Fukushima University, Kanayagawa, Fukushima 960-1296, Japan
[b] Department of Environmental Science, Faculty of Education, Fukushima University, Kanayagawa, Fukushima 960-1296, Japan

Received 8 March 2005; accepted 26 April 2005
Available online 13 June 2005

Ruthenium and Osmium Chemistry Topical Issue

Abstract

Ruthenium phosphine complexes with a CO ligand $[Ru(tpy)(PR_3)(CO)Cl]^+$ (tpy = 2,2′:6′,2″-terpyridine, R = Ph or *p*-tolyl), were prepared by introduction of CO gas to the corresponding dichloro complexes at room temperature. New carbonyl complexes were characterized by various methods including structural analyses. They were shown to release CO following the addition of several N-donors to form the corresponding substituted complexes. The kinetic data and structural results observed in this study indicated that the CO release reactions proceeded in an interchange mechanism. The molecular structures of $[Ru(tpy)(PPh_3)(CO)Cl]PF_6$, $[Ru(tpy)(P(p\text{-tolyl})_3)(CO)Cl]PF_6$ and $[Ru(tpy)(PPh_3)(CH_3CN)Cl]PF_6$ were determined by X-ray crystallography.

Keywords: Ruthenium; Carbonyl; Polypyridyl complexes; Crystal structures; CO-release reaction; Reaction mechanism

1. Introduction

For several reasons, we have recently developed an increasing interest in the analysis of the bond characteristics of polypyridyl ruthenium(II) complexes involving carbonyl ligands. The bond scission of ruthenium–carbon in Ru–CO moiety is a key reaction in utilizing polypyridyl ruthenium(II) complexes as catalysts for the reduction of carbon dioxide [1]. Synthesis of complexes capable of CO release is needed to investigate the biological activities of CO because it is known that CO gas is generated in the human body and plays an important role [2].

In general, polypyridyl ruthenium (II) carbonyl complexes are kinetically inert for CO release since they are usually saturated 18-electron complexes. Therefore, reactions to remove CO ligands are carried out using reagents such as $NaBH_4$ [3], redox reactions [4], or photoirradiation [5]. On the other hand, some studies reported that coligands on other ruthenium(II) carbonyl systems facilitate a Ru–CO bond breaking through steric and electronic effects [6]. Such studies gave us some ideas to achieve the lability of inert Ru–CO bond without reagents or redox/photo reactions. That is, the design of complexes considering their steric and electron donor/acceptor effects of coligands may allow the systematic control of Ru–CO bond strength in polypyridyl ruthenium(II) carbonyl complexes system.

* Corresponding author. Tel./fax: +81 24 548 8199.
E-mail address: ooyama@sss.fukushima-u.ac.jp (D. Ooyama).

0020-1693/$ - see front matter © 2005 Elsevier B.V. All rights reserved.
doi:10.1016/j.ica.2005.04.040

In the present study, we introduced two kinds of phosphorous compounds (PPh_3 and P(*p*-tolyl)$_3$) as candidates for achieving the lability of Ru–CO bond to the *trans* position of a CO ligand and constructed a suitable complex system (*trans*(CO,PR_3)-[Ru(tpy)(PR_3)(CO)Cl]$^+$: tpy = 2,2′:6′,2″-terpyridine; R = phenyl, *p*-tolyl). We further reported kinetic investigations to determine the CO dissociation rate and mechanistic assignments using several N-donor compounds which can coordinate with the ruthenium(II) center.

2. Experimental

2.1. Physical and kinetic measurements

Elemental analyses were carried out at the Research Center for Molecular-Scale Nanoscience, Institute for Molecular Science. IR spectra were obtained on KBr pellets or in CH_3CN solution (window: KRS-5) with a Shimadzu FT-IR 8100 spectrometer. ESI-MS were obtained with a Shimadzu LC-MS 2100 mass spectrometer. UV–Vis spectra were obtained with an Ocean Optics S2000 fiber optics spectrometer equipped with an Analytical Instrument Systems light source. Kinetic measurements were carried out at 25(1) °C in a constant temperature room. Stock solutions of [Ru(tpy)(PPh_3)(CO)Cl]$^+$ and [Ru(tpy)(P(*p*-tolyl)$_3$)(CO)Cl]$^+$ were prepared in 1,2-dichloroethane (DCE) under N_2. Each complex concentration was 1.0×10^{-4} mol dm^{-3}. Liquid entering ligands (acetonitrile, benzonitrile and propionitrile) were added using a syringe to the solution of the carbonyl complexes. A portion of the mixed solution was transferred by syringe to the UV–Vis spectral cell and the spectrum of the sample was recorded at appropriate intervals. For the determination of k_{obs} the increase in absorption (A_t) at 460–470 nm corresponding to the substituted species was recorded as a function of time (t). A_∞ was measured when the intensity changes leveled off. Values of pseudo-first order rate constants were obtained from the slopes of linear least-squares plots of $-\ln(A_\infty - A_t)$ against t [7].

2.2. Preparation of complexes

[Ru(PPh_3)$_3$Cl$_2$], [Ru(P(*p*-tolyl)$_3$)$_3$Cl$_2$], [Ru(tpy)(PPh_3)Cl$_2$], and [Ru(tpy)(P(*p*-tolyl)$_3$)Cl$_2$] were prepared according to procedures outlined elsewhere [8,9].

2.2.1. *trans*(CO,PPh_3)-[Ru(tpy)(PPh_3)(CO)Cl]PF_6

A CH_2Cl_2 solution (40 cm^3) of *cis*(Cl)-[Ru(tpy)(PPh_3)Cl$_2$] (40 mg) was stirred at room temperature under 10 atm of CO for 6 h. Once the reaction mixture was concentrated under reduced pressure, crystals were precipitated by the addition of ether. An aqueous KPF_6 solution was added to a methanolic solution of the crude product, and then the precipitate was collected to give [Ru(tpy)(PPh_3)(CO)Cl]PF_6 with a 66% yield. IR (KBr): 2008 cm^{-1} ν(C≡O). ESI-MS: m/z = 632 ([M − CO]$^+$). *Anal.* Calc. for $C_{34}H_{26}N_3OF_6ClP_2Ru$: C, 50.73; H, 3.26; N, 5.22. Found: C, 50.77; H, 3.26; N, 5.22%.

2.2.2. *trans*(CO,P(*p*-tolyl)$_3$)-[Ru(tpy)(P(*p*-tolyl)$_3$)(CO)Cl]PF_6

A similar reaction between *cis*(Cl)-[Ru(tpy)(P(*p*-tolyl)$_3$)Cl$_2$] and CO gas under the same conditions described above gave rise to [Ru(tpy)(P(*p*-tolyl)$_3$)(CO)Cl]PF_6 with 77% yield. IR (KBr): 2004 cm^{-1} ν(C≡O). ESI-MS: m/z = 674 ([M − CO]$^+$). *Anal.* Calc. for $C_{37}H_{32}N_3OF_6ClP_2Ru$: C, 52.46; H, 3.81; N, 4.96. Found: C, 52.56; H, 3.81; N, 4.99%.

2.3. CO-release of [Ru(tpy)(PR_3)(CO)Cl]PF_6 (R = Ph or p-tolyl) in acetonitrile solution: isolation of *trans*(Cl,PR_3)-[Ru(tpy)(PR_3)(CH_3CN)Cl]PF_6 (R = Ph or p-tolyl)

Either of the complexes [Ru(tpy)(PPh_3)(CO)Cl]PF_6 or [Ru(tpy)(P(*p*-tolyl)$_3$)(CO)Cl]PF_6 (30 mg) were dissolved in CH_3CN (2 cm^3) at room temperature in the dark. The solution was stirred for 4 days and then ether (3 cm^3) was added into the solution at 4 °C. Orange crystals of [Ru(tpy)(PPh_3)(CH_3CN)Cl]PF_6 or [Ru(tpy)(P(*p*-tolyl)$_3$)(CH_3CN)Cl]PF_6 gradually appeared out of the solution. The yield of [Ru(tpy)(PPh_3)(CH_3CN)Cl]PF_6 was 85%. ESI-MS: m/z = 673 ([M]$^+$), 632 ([M − CH_3CN]$^+$). *Anal.* Calc. for $C_{35}H_{29}N_4F_6ClP_2Ru$: C, 51.38; H, 3.57; N, 6.85. Found: C, 51.16; H, 3.65; N, 6.85%. The yield of [Ru(tpy)(P(*p*-tolyl)$_3$)(CH_3CN)Cl]PF_6 was 87%. ESI-MS: m/z = 715 ([M]$^+$), 674 ([M − CH_3CN]$^+$). *Anal.* Calc. for $C_{38}H_{35}N_4F_6ClP_2Ru$: C, 53.06; H, 4.10; N, 6.51. Found: C, 52.92; H, 4.17; N, 6.45%.

2.4. X-ray crystallography

Crystallographic data for [Ru(tpy)(PPh_3)(CO)Cl]PF_6, [Ru(tpy)(P(*p*-tolyl)$_3$)(CO)Cl]PF_6 and [Ru(tpy)(PPh_3)(CH_3CN)Cl]PF_6 are summarized in Table 1. Data for these complexes were collected on a Rigaku/MSC Mercury CCD diffractometer with graphite monochromated Mo Kα radiation (λ = 0.71070 Å) at −100 °C. Data were collected to a maximum of 2θ value of 55.0°. A total of 720 oscillation images were collected. All calculations were carried out on a workstation of Silicon Graphics Corporation, using the TEXSAN crystallographic software package of the Molecular Structure Corporation. The structures were solved either by the Patterson method ([Ru(tpy)(PPh_3)(CO)Cl]PF_6 and [Ru(tpy)(P(*p*-tolyl)$_3$)(CO)Cl]PF_6) [10] or by a direct method ([Ru(tpy)(PPh_3)(CH_3CN)Cl]PF_6) [11] and were expanded using Fourier techniques. Empirical absorp-

Table 1
Crystallographic data for $[Ru(tpy)(PPh_3)(CO)Cl]PF_6$, $[Ru(tpy)(P(p\text{-tolyl})_3)(CO)Cl]PF_6$ and $[Ru(tpy)(PPh_3)(CH_3CN)Cl]PF_6$

Chemical formula	$C_{34}H_{26}N_3OF_6ClP_2Ru$	$C_{37}H_{32}N_3OF_6ClP_2Ru$	$C_{35}H_{29}N_4F_6ClP_2Ru$
Formula weight	805.06	847.14	818.10
Temperature (K)	173	173	173
Crystal system	monoclinic	monoclinic	monoclinic
Space group	$P2_1/c$	$P2_1/c$	$P2_1/n$
Unit cell parameters			
a (Å)	10.5843(5)	14.796(8)	13.323(4)
b (Å)	14.5950(8)	13.937(7)	26.363(7)
c (Å)	21.086(3)	18.55(1)	19.652(6)
β (°)	91.523(2)	109.027(7)	92.529(4)
V (Å^3)	3256.1(3)	3616(3)	6896(3)
Z	4	4	8
μ(Mo Kα) (cm^{-1})	7.30	6.62	6.90
Number of reflections measured	7701	8508	16103
Number of observations	7402 (all)	8175 (all)	15751 (all)
Parameters	433	460	883
$R1$[a]	0.046	0.083	0.083
R_w[b]	0.107 (all data)	0.148 (all data)	0.159 (all data)
S	1.40	1.23	1.62

[a] $R = \sum||F_o|-|F_c||/\sum|F_o|$.
[b] $R_w = \{\sum_w(F_o^2 - F_c^2)^2/\sum_w(F_o^2)^2\}^{1/2}$.

tion corrections were applied using Lorentz polarization (Lp) and absorption. Structures were refined with the full-matrix least-square techniques. The non-hydrogen atoms were refined anisotropically, and hydrogen atoms were placed in idealized positions. The final cycle of full-matrix least-squares refinements was based on 7402 observations (all data), 433 variable parameters for $[Ru(tpy)(PPh_3)(CO)Cl]PF_6$, 8175 and 460 for $[Ru(tpy)(P(p\text{-tolyl})_3)(CO)Cl]PF_6$, and 15751 and 883 for $[Ru(tpy)(PPh_3)(CH_3CN)Cl]PF_6$, respectively.

3. Results and discussion

3.1. Syntheses and characterization of carbonyl complexes

We synthesized the desirable complexes to labilize the Ru–CO bond: ruthenium complexes contained both a CO and a π-acidic phosphine compound at the *trans* position mutually. In Scheme 1, the implied difference in synthesis is shown. In pass (a), the precursors *cis*(Cl)-$[Ru(tpy)(PR_3)Cl_2]$ react with CO in DCE at reflux to give *cis*(Cl)-$[Ru(tpy)(CO)Cl_2]$ [9], whereas they undergo a chloride substitution reaction with CO gas under high-pressure at room temperature to form *trans*(CO,PR_3)-$[Ru(tpy)(PR_3)(CO)Cl]^+$ in pass (b).

These carbonyl complexes were characterized by various measurements. ESI-mass spectra in CH_3CN solution showed the main peaks (m/z : 632 for R = Ph, 674 for R = *p*-tolyl, respectively) together with the isotope distribution pattern of ruthenium nuclei. These peak values corresponded to CO-loss forms. IR spectra of the complexes displayed a strong band ν(C≡O) at

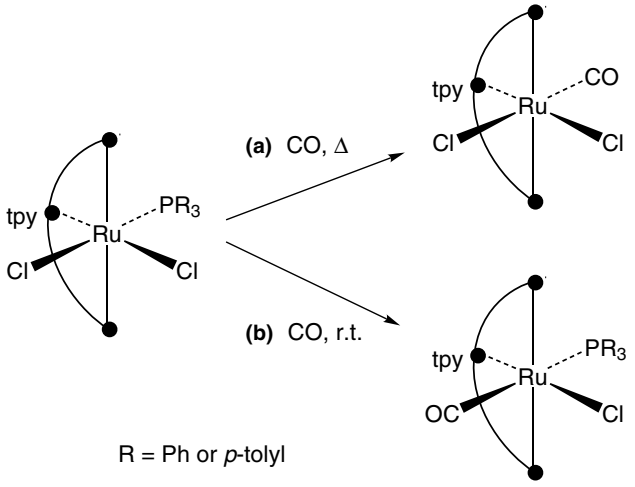

Scheme 1.

2008 (for R = Ph) and 2004 cm^{-1} (for R = *p*-tolyl), respectively. The 2008 cm^{-1} value in R = Ph, is 51 cm^{-1} higher than that of the corresponding chloro complex (1957 cm^{-1}) [9] due to the existence of more electron-accepting phosphine ligand *trans* to CO. A single ν(C≡O) band also displayed no other isomers in these complexes.

Figs. 1 and 2 display the molecular structures of R = Ph and *p*-tolyl, respectively. Selected bond lengths and angles are listed in Table 2. The coordinating environments around the ruthenium atom of both R = Ph and *p*-tolyl were essentially the same: each complex had a distorted octahedral geometry with three nitrogen atoms of the tpy ligand, one phosphorous atom, one chloride ion and one carbon at the terminal carbonyl group. The carbonyl ligand was at the *trans* position

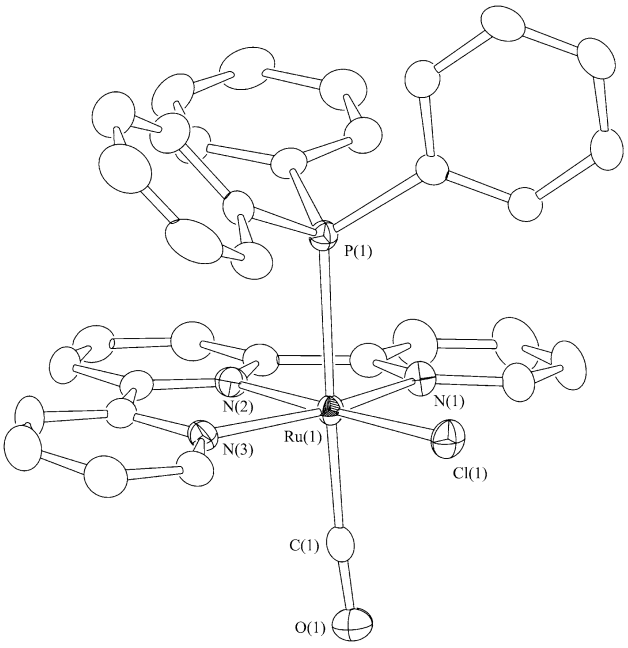

Fig. 1. An ORTEP view of $[Ru(tpy)(PPh_3)(CO)Cl]^+$ with atom labeling. Hydrogen atoms are omitted for clarity. The thermal ellipsoids are shown at the 50% probability level.

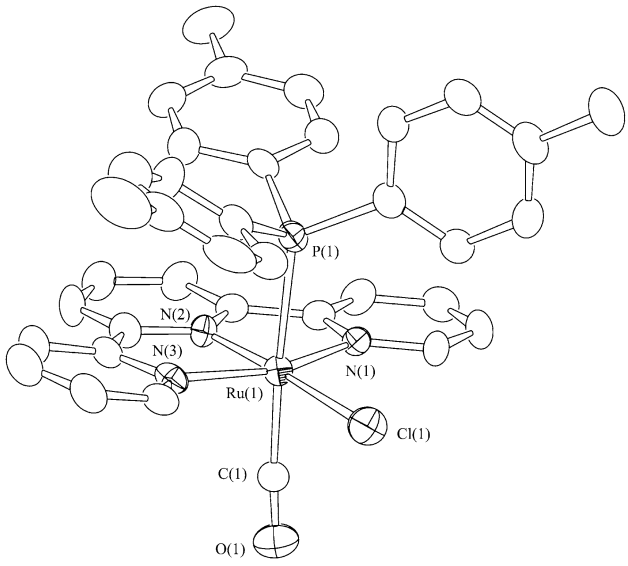

Fig. 2. An ORTEP view of $[Ru(tpy)(P(p\text{-tolyl})_3)(CO)Cl]^+$ with atom labeling. Hydrogen atoms are omitted for clarity. The thermal ellipsoids are shown at the 50% probability level.

with respect to the phosphine. The Ru–P bond lengths of R = Ph and *p*-tolyl (2.4811(7) and 2.467(2) Å, respectively) were in the range of those of Ru(II)–phosphine complexes [12]. The bond lengths of the three Ru–N in R = Ph (2.102(2), 1.978(2) and 2.082(2) Å) were comparable to those of R = *p*-tolyl (2.097(4), 1.974(4) and 2.089(4) Å). These lengths are typical in the structure of other Ru(II) complexes with terpyridine [13]. The bond lengths of Ru–Cl (2.4228(7) and 2.425(1) Å, respectively) were also in the range of those of Ru(II)–terpyridine–chloro complexes [13]. Both Ru–CO units were essentially linear with the ruthenium atom (175.6(2)° for R = Ph, 174.7(5)° for R = *p*-tolyl, respectively) and the Ru–C and the C–O bond lengths (1.891(3) and 1.138(3) Å, respectively for R = Ph, 1.897(5) and 1.134(6) Å, respectively, for R = *p*-tolyl) were similar to typical values in other Ru(II) carbonyl complexes [1].

3.2. Ru–CO bond lability in the complexes: CO-release behavior in solutions

The UV–Vis spectrum of $[Ru(tpy)(PR_3)(CO)Cl]^+$ showed a weak MLCT band at 405 nm ($\varepsilon = 3.2 \times 10^3$ dm^3 mol^{-1} cm^{-1}) for R = Ph and 407 nm ($\varepsilon = 3.0 \times 10^3$ dm^3 mol^{-1} cm^{-1}) for R = *p*-tolyl in DCE.

Table 2
Selected bond lengths (Å) and angles (°) for $[Ru(tpy)(PPh_3)(CO)Cl]PF_6$, $[Ru(tpy)(P(p\text{-tolyl})_3)(CO)Cl]PF_6$ and $[Ru(tpy)(PPh_3)(CH_3CN)Cl]PF_6$

$[Ru(tpy)(PPh_3)(CO)Cl]^+$		$[Ru(tpy)(P(p\text{-tolyl})_3)(CO)Cl]^+$		$[Ru(tpy)(PPh_3)(CH_3CN)Cl]^+$	
Bond lengths					
Ru1–P1	2.4811(7)	Ru1–P1	2.467(2)	Ru1–P1	2.312(1)
Ru1–Cl1	2.4228(7)	Ru1–Cl1	2.425(1)	Ru1–Cl1	2.446(1)
Ru1–C1	1.891(3)	Ru1–C1	1.897(5)	Ru1–N1	2.095(4)
Ru1–N1	2.102(2)	Ru1–N1	2.097(4)	Ru1–N2	1.954(3)
Ru1–N2	1.978(2)	Ru1–N2	1.974(4)	Ru1–N3	2.079(4)
Ru1–N3	2.082(2)	Ru1–N3	2.089(4)	Ru1–N4	2.063(4)
C1–O1	1.138(3)	C1–O1	1.134(6)	N4–C16	1.380(5)
				C16–C17	1.448(6)
Bond angles					
N1–Ru1–N2	79.27(9)	N1–Ru1–N2	79.3(2)	N1–Ru1–N2	79.6(1)
N2–Ru1–N3	79.48(10)	N2–Ru1–N3	79.4(2)	N2–Ru1–N3	79.9(1)
P1–Ru1–Cl1	89.11(2)	P1–Ru1–Cl1	91.59(5)	P1–Ru1–Cl1	176.23(4)
P1–Ru1–C1	177.02(8)	P1–Ru1–C1	175.2(2)	P1–Ru1–N4	97.1(1)
Cl1–Ru1–C1	87.91(8)	Cl1–Ru1–C1	83.6(2)	Cl1–Ru1–N4	84.6(1)
Ru1–C1–O1	175.6(2)	Ru1–C1–O1	174.7(5)	Ru1–N4–C16	164.6(4)
				N4–C16–C17	176.9(5)

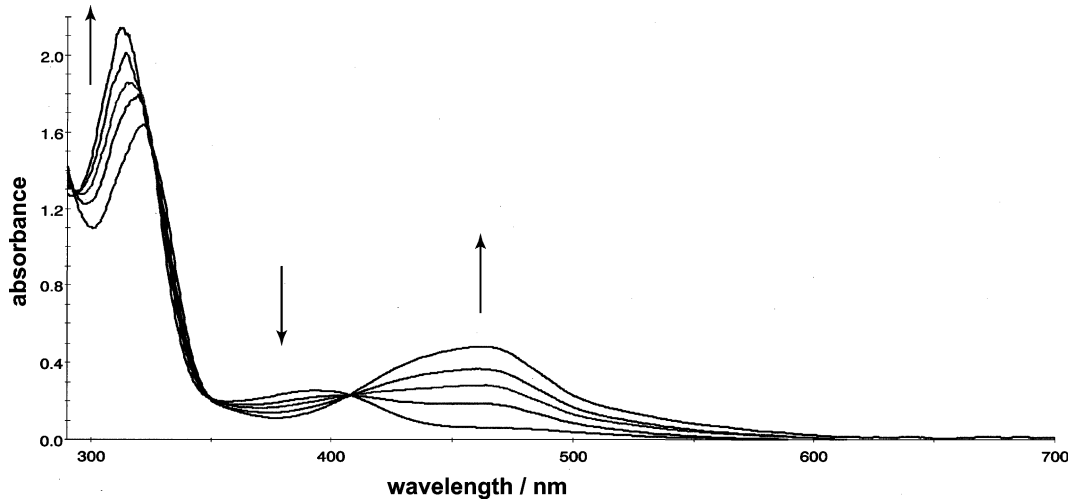

Fig. 3. Time dependence of the electronic spectra of $[Ru(tpy)(PPh_3)(CO)Cl]^+$ in CH_3CN at 25 °C (1.0×10^{-4} mol dm^{-3}).

No spectral change was observed in both complexes after 1 day. On the other hand, the light orange PPh_3 complex solution gradually changed to a deep orange color when the complex was dissolved in CH_3CN in the dark (Fig. 3). The original band at 405 nm gradually decreased with time, and new bands increased at 320 and 466 nm with the isosbestic points. The solution IR spectrum after this reaction showed the disappearance of the characteristic peak of the terminal CO triple bond. Therefore, it is suggested that this was a substitution reaction between the coordinated carbonyl and an acetonitrile (solvent)

$$[Ru(tpy)(PR_3)(CO)Cl]^+ + R'CN \xrightarrow{k_{obs}} [Ru(tpy)(PR_3)(R'CN)Cl]^+ + CO \quad (1)$$

The kinetics of the reactions shown in Eq. (1) have been monitored by UV–Vis spectroscopy to determine the rate constants and to obtain mechanistic evidences.

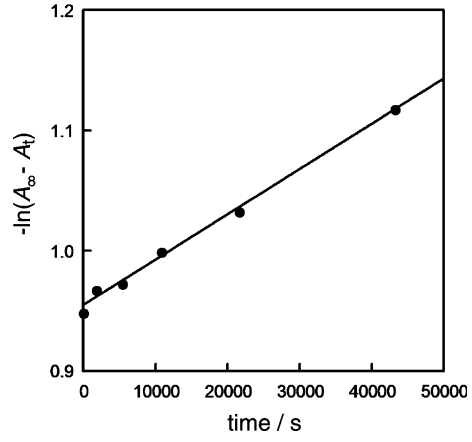

Fig. 4. Plots of ln(Δabsorbance) vs. time for the reaction of $[Ru(tpy)(PPh_3)(CO)Cl]^+$ (1.0×10^{-4} mol dm^{-3}) with CH_3CN (0.02 mol dm^{-3}) in DCE at 25 °C.

Examples of ln(Δabsorbance) versus time plots are shown in Fig. 4 for the reaction with acetonitrile (0.02 mol dm^{-3} in DCE). Fig. 4 indicates that this reaction allows for a first-order rate constant k_{obs}. In addition, the reaction was studied using different concentrations or kinds of entering ligands (R′CN). In principle, the rate constants k_{obs} are pseudo-first order because the entering ligand concentrations (>0.01 mol dm^{-3}) were always larger than that of $[Ru(tpy)(PR_3)(CO)Cl]^+$ (<1×10^{-4} mol dm^{-3}). We found that the rates for all of the reactions were independent of the concentration of acetonitrile (Table 3). This tendency was established for concentrations of acetonitrile between 0.01 and 0.05 mol dm^{-3} in DCE. Therefore, the rate law for the Eq. (1) is given by

$$\text{rate} = k_{obs}[Ru(tpy)(PR_3)(CO)Cl]. \quad (2)$$

Additionally, the value of k_{obs} was found to be independent of the nature of the entering ligands (R′CN) including their basicity and steric requirements (Table 3). As a result, this system is consistent with a dissociative mechanism rather than an associative one. Similarly, $[Ru(tpy)(P(p\text{-tolyl})_3)(CO)Cl]^+$ also indicated CO dissociation. Taking into account the stability of the Ru–CO bond in the analogous complexes *trans*- and *cis*(Cl)-

Table 3
Summary of PR_3 properties and CO-release rate constants for $[Ru(tpy)(PR_3)(CO)Cl]^+$ (R = Ph or *p*-tolyl)

R	pK_a[a]	Cone angle[b]	[R′CN] (mol dm^{-3})	10^6k (s^{-1})		
				R′ = Me	R′ = Et	R′ = Ph
Ph	2.73	145°	0.01	4.00	4.56	5.01
			0.02	3.76		
			0.05	4.80		
p-Tolyl	3.84	145°	0.01	5.85		

[a] Ref. [15].
[b] Ref. [16].

$[Ru(tpy)(CO)Cl_2]$ [9], it is suggested that the selection of this configuration and the phosphine ligands make the Ru–CO lability possible. In general, ligands with electron-donating substituents are strong donors. Thus, $P(p\text{-tolyl})_3$ donates more strongly than PPh_3 to the ruthenium. As a result, $[Ru(tpy)(P(p\text{-tolyl})_3)(CO)Cl]^+$ is more electron-rich than $[Ru(tpy)(PPh_3)(CO)Cl]^+$ and therefore the former is considered to have stronger basicity [14]. However, both complexes showed a similar rate constant (Table 3). These results indicated that the Ru–C bond strength was minimally affected by the small difference of pK_a values. Therefore, systematic preparation of complexes containing suitable ligands (with much higher or lower pK_a's for phosphines compared with the present ones) may be required for a better discussion on the relationship between Ru–C bond strengths and ligand basicities.

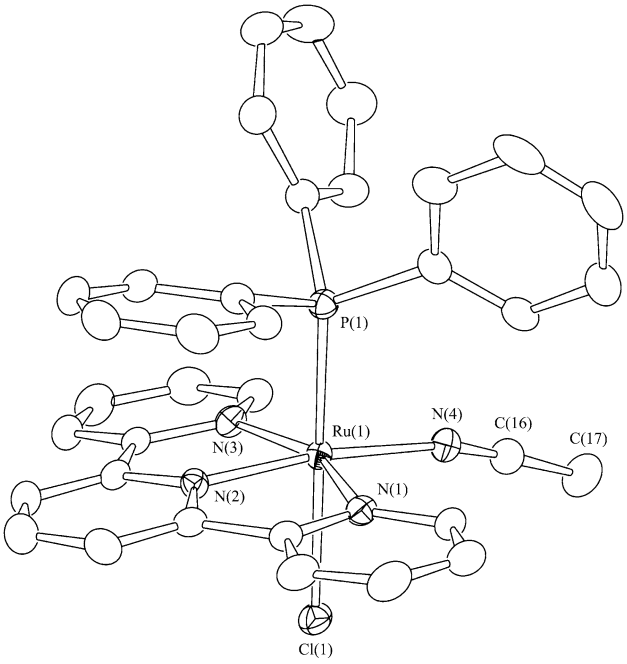

Fig. 5. An ORTEP view of $[Ru(tpy)(PPh_3)(CH_3CN)Cl]^+$ with atom labeling. Hydrogen atoms are omitted for clarity. The thermal ellipsoids are shown at the 50% probability level.

3.3. Isolation of the substituted complexes: CO-release reaction with steric change

We quantitatively isolated the substituted complexes from each solution and attempted to characterize them. The CO stretching band disappeared from the IR measurements. From ESI-MS measurements, the compounds were characterized as the corresponding solvent complexes, $[Ru(tpy)(PR_3)(R'CN)Cl]PF_6$ (R = Ph or *p*-tolyl; R′ = Me, Et or Ph). In addition, the acetonitrile complexes $[Ru(tpy)(PPh_3)(CH_3CN)Cl]^+$ and $[Ru(tpy)(P(p\text{-tolyl})_3)(CH_3CN)Cl]^+$, were characterized by elemental analyses (see Experimental section). The crystal structure was determined using a suitable crystal in $[Ru(tpy)(PPh_3)(CH_3CN)Cl]PF_6$. Interestingly, it was confirmed that an acetonitirile molecule attached to the *cis* position with respect to the phosphine ligand, which was different from the dissociated CO position (Fig. 5). We suggested that an interchange mechanism (I-mechanism) rather than a simple dissociative one (D-mechanism) was employed due to steric change accompanying the CO-release reaction [17]. Scheme 2 shows the possible mechanism of the CO-release reaction. It is possible that the entering ligands (R′CN) attack to the ruthenium center from the phosphine side rather than the CO side. Results from the structural studies apparently supported the assumption that the reaction proceeded via I-mechanism.

On the other hand, when CO was introduced into the formed complexes, $[Ru(tpy)(PR_3)(CH_3CN)Cl]^+$, the original carbonyl complexes with the same configuration were reproduced (by IR and ^1H NMR spectra). As shown in Scheme 3, the results obtained led to the

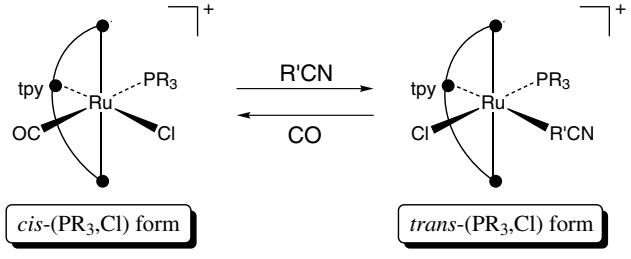

Scheme 3.

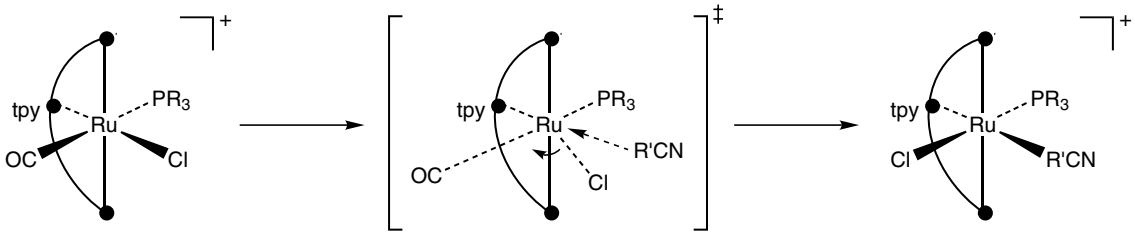

Scheme 2.

conclusion that CO loss/uptake controls the steric configuration of the complex.

4. Conclusion

From this study, we can conclude that the selection and introduction of phosphine ligands allows labilization of the Ru–CO bond, which results in the regulation of reactivity of the compounds in biological or catalytic processes. The present topic will be addressed in a future publication on the reactivity of $[Ru(tpy)(PR_3)(CO)Cl]^+$ having various phosphines.

5. Supplementary material

Crystallographic data for structural analysis have been deposited with the Cambridge Crystallographic Data Centre, CCDC Nos. 254144 for $[Ru(tpy)(PPh_3)(CO)Cl]PF_6$, 258940 for $[Ru(tpy)(P(p\text{-tolyl})_3)(CO)Cl]PF_6$ and 254145 for $[Ru(tpy)(PPh_3)(CH_3CN)Cl]PF_6$, respectively. Copies of this information may be obtained free of charge from The Director, CCDC, 12 Union Road, Cambridge CB2 1EZ, UK.

Acknowledgments

We are indebted to Professor Koji Tanaka of the Institute for Molecular Science for his helpful advice and discussion. We thank Dr. Kazushi Shiren for performing the X-ray measurements. This work was supported by the Joint Studies Program (2003–2004) of the Institute for Molecular Science.

References

[1] (a) D. Ooyama, T. Tomon, K. Tsuge, K. Tanaka, J. Organomet. Chem. 619 (2001) 299;
(b) K. Tanaka, D. Ooyama, Coord. Chem. Rev. 226 (2002) 211.
[2] (a) A. Verma, D.J. Hirsch, C.E. Glatt, G.V. Ronnett, S.H. Synder, Science 259 (1993) 381;
(b) M.D. Maines, Mol. Cell Neurosci. 4 (1993) 389;
(c) T. Ingi, J. Cheng, G.V. Ronnett, Neuron 16 (1996) 835.
[3] H. Nagao, T. Mizukawa, K. Tanaka, Inorg. Chem. 33 (1994) 3415.
[4] K. Tanaka, Bull. Chem. Soc. Jpn. 71 (1998) 17.
[5] J.L. Hughey, C.R. Bock, T.J. Meyer, J. Am. Chem. Soc. 97 (1975) 4440.
[6] J. Pearson, J. Cooke, J. Takats, R.B. Jordan, J. Am. Chem. Soc. 120 (1998) 1434.
[7] A.W. Zanella, P.C. Ford, Inorg. Chem. 14 (1975) 42.
[8] P.S. Hallman, T.A. Stephenson, G. Wilkinson, Inorg. Synth. 12 (1970) 237.
[9] B.P. Sullivan, J.M. Calvert, T.J. Meyer, Inorg. Chem. 19 (1980) 1404.
[10] PATTY: P.T. Beurskens, G. Admiraal, G. Beurkens, W.P. Bosman, R. de Gelder, R. Israel, J.M.M. Smith, The DIRDIF-94 program system, Technical Report of the Crystallography Laboratory; University of Nijmengen, The Netherlands, 1994.
[11] SIR-92: A. Altomare, M. Cascarano, C. Giacovazzo, A. Guagliardi, J. Appl. Crystallogr. 26 (1993) 343.
[12] (a) J.C. Jeffrey, T.B. Rauchfuss, Inorg. Chem. 18 (1979) 2658;
(b) K.D. Schramm, J.A. Ibers, Inorg. Chem. 19 (1980) 2441.
[13] (a) M.-H.V. Huynh, J. Smyth, M. Welzler, B. Mort, P.K. Gong, L.M. Witham, D.L. Jameson, D.K. Geiger, J.M. Lasker, M. Charepoo, M. Gornikiewicz, J.M. Cintron, G. Imahori, R.R. Sanchez, A.C. Marschilok, L.M. Krajkowski, D.G. Churchill, M.R. Churchill, K.J. Takeuchi, Angew. Chem. Int. Ed. Engl. 40 (2001) 4469;
(b) C.M. Hartshorn, K.A. Maxwell, P.S. White, J.M. DeSimone, T.J. Meyer, Inorg. Chem. 40 (2001) 601;
(c) C. Bonnefous, A. Chouai, R.P. Thummel, Inorg. Chem. 40 (2001) 5851;
(d) B. Mondal, M.G. Walawalkar, G.K. Lahiri, J. Chem. Soc., Dalton Trans. (2000) 4209;
(e) V.J. Catalano, R.A. Heck, C.E. Immoos, A. Öhma, M.G. Hill, Inorg. Chem. 37 (1998) 2150;
(f) L.F. Szczepura, S.M. Maricich, R.F. See, M.R. Churchill, K.J. Takeuchi, Inorg. Chem. 34 (1995) 4198;
(g) A.L. Spek, A. Gerli, J. Reedijk, Acta Crystallogr., Sect. C 50 (1994) 394.
[14] S. Komiya (Ed.), Synthesis of Organometallic Compounds, John Wiley & Sons, Chichester, 1997, p. 27.
[15] C.A. Tolman, Chem. Rev. 77 (1977) 313.
[16] M.N. Golovin, M.M. Rahman, J.E. Belmonte, W.P. Giering, Organometallics 4 (1985) 1981.
[17] G.L. Miesller, D.A. Tarr, Inorganic Chemistry, Japanese ed., Maruzen, Tokyo, 2003, p. 524.